RESEARCH REPORT RR-016

RR-16

VERTICAL MOTION IN THE INDIAN SUMMER MONSOON

by

S.T. AWADE AND R. N. KESHAVAMURTY

NDIAN INSTITUTE OF TROPICAL METEOROLOGY

Ramdurg House
Ganeshkhind Road
Poona-5, India

August 1974

RR-16

Vertical motion in the Indian summer monsoon

By

S.T. Awade and R.N. Keshavamurty
Indian Institute of Tropical Meteorology, Poona - 5.

Abstract :

The vertical motion field in the Indian monsoon region has been studied for mean July, a strong monsoon day and a weak monsoon day. We have used quasi-geostrophic ω -equation for this purpose. Besides the forcings due to thermal and differential vorticity advection, the vertical motion due to orography and friction have also been included. The vertical motion due to the various forcings have been partitioned. The ω- fields due to all forcings, due to individual forcings and their vertical profiles are delineated.

Conversion from potential to kinetic energy associated with the vertical circulations have also been computed and presented.

Introduction :

Estimates of conversion from potential into kinetic energy involve the vertical 'p' velocity. Vertical motion fields and associated circulations in the monsoon have been discussed by Das (1962), Saha (1968), Koteswaram (1960), Rao (1962), Asnani* and Keshavamurty (1971). Vertical motion fields in association with monsoon depressions have been studied by Rao and Rajamani (1968). In this paper we have computed vertical motion fields in the Indian monsoon region during mean July and two contrasting monsoon situations, using quasi-geostrophic ω equation with friction and orography.

2. Data and computations :

Quasi-geostrophic ω and energy conversions have been computed for mean July, on a strong monsoon day i.e. 7 July 1963 and on a weak monsoon day i.e. 19 July 1963. These situations were earlier studied by Raman et al (1965). Fig. 1 (a, b) show the 1000 mb charts for these two dates. It is seen that the monsoon trough has shifted to the foot of the Himalayas on the weak monsoon day.

We have used height data at 1000, 850, 700, 500, 300, 200 and 100 mb and have computed ω at 850, 700, 500, 300, and 200 mb.

The area for which computations are made is from 5° N to 22.5° N and 55° E to 95° E.

---

* personal communication

3. Quasi-geostrophic ω -equation :

The vorticity equation is given by

$$\frac{\partial \xi}{\partial t} + \mathbb{V}.\nabla\ (\xi + f) = f_o \frac{\partial \omega}{\partial p} \qquad \cdots (1)$$

The thermodynamic energy equation for adiabatic motion is given by

$$\frac{\partial}{\partial t}\left(\frac{\partial \phi}{\partial p}\right) + \mathbb{V}.\nabla\left(\frac{\partial \phi}{\partial p}\right) + \sigma\omega = 0 \qquad \cdots (2)$$

$$\xi = \frac{1}{f_o}\nabla^2\phi = \nabla^2\psi \qquad \cdots (3)$$

$$\sigma = -\frac{\alpha}{\theta}\frac{\partial \theta}{\partial p} \qquad \cdots (4)$$

$$\mathbb{V} = \mathbb{K} \times \frac{g}{f}\nabla z \qquad \cdots (5)$$

The static stability parameter is taken as constant in any isobaric surface i.e. $\sigma = \sigma(p)$

Using equation (1) and (2) we obtain the quasi-geostrophic ω equation

$$\sigma\nabla^2\omega + f_o^2\frac{\partial^2\omega}{\partial p^2} = g\frac{\partial}{\partial p}J(z,\eta) - \frac{g^2}{f_o}\nabla^2 J\left(z, \frac{\partial z}{\partial p}\right) \cdots (6)$$

$$\eta = \frac{g}{f_o}\nabla^2 z + f \qquad \cdots (7)$$

The equation (6) is the quasi-geostrophic omega equation. The first term on the right hand side of in equation (6) is the forcing due to vorticity advection and the second term is the forcing due to thermal advection. These forcing can be calculated from a given height field.

We have solved this equation by relaxation. At the side walls and at the top the boundary condition used is $\omega = 0$. At the bottom, we have used ω due to friction and orography.

... 4

We have used Charney and Eliassen's formula (1949) for frictional ω . Using Ekman theory of airflow in the frictional layer, frictional ω at the top of frictional layer is given by

$$\omega_F = - g\rho\sqrt{\frac{k}{2f_0}} \sin 2\alpha \; (\xi_{g\,1000})$$

k = coefficient of eddy viscosity

= $10 m^2 sec^{-1}$

α = $22\frac{1}{2}$, angle or inflow

ρ = air density in Ekman layer assumed constant

= 1.0625×10^3 gm m^{-3}

$\xi_{g\,1000}$ = Geostrophic vorticity at 1000 mb

$f_0 = f_{15^\circ N} = 3.775 \times 10^{-5}$ sec^{-1}, coriolis parameter at latitude 15° N.

The orographic ω was obtained by

$\omega_0 = - g\rho(\mathbb{V}_{g\,1000} . \nabla h)$ where h is the height of terrain above sea level taken from Berkofsky and Bertoni (1960)

Since the above ω equation is linear, we can partition the ω due to different forcing and also due to different boundary conditions.

4. Results and Discussion :

Fig. 2 (a,b,c,d,e) show the field of ω for mean July at 850, 700, 500, 300 and 200 mb. At 850 mb there are two centres of upward motion, one over east Madhya Pradesh and Orissa and another of Saurashtra, Konkan coasts. These regions of upward motion extend to 300 mb over east MP and to 500 mb and over NE Arabian sea respectively. There is a region of descent over Central Arabian sea at 850 mb. There is a region of descent over east Arabian sea from

700 to 200 mb. At 500, 300 mb and 200 mb an east-west circulation with ascent over Andaman sea and descent over East Arabian sea is seen.

Fig. 3 (a,b,c,d,e) show similar ω -charts for 7 July 1963, which was an active monsoon day (for the same levels). At 850 mb we have a region of strong ascent over West Madhya Pradesh and neighbourhood. This was in association with a depression. There is ascent over North Arabian sea also in connection with the midtropospheric system. These regions of ascent are seen at 700 mb also. There is a region of strong descent south peninsula from 850 to 300 mb.

Fig. 4 (a,b,c,d,e) show similar charts for 19 July 1963, a weak monsoon day, when the monsoon trough had shifted to the foot of the Himalayas. Except for a region of ascent over Gujarat at 850 mb generally descending motion is noticed throughout.

Let us now look at the partitioned ω's due to the various forcings on 7 July 1963. Fig. 5 (a,b,c,d,e) and 6 (a,b,c,d,e) show the partitioned ω due to thermal advection and vorticity advection respectively for 7th July 1963. It is seen that the descent over south peninsula is mainly due to thermal advection (apart from orography). Over south peninsula at 850 mb ω due to thermal and vorticity advection oppose each other. It is generally seen that the ω (due to dynamical forcing) fall off with increasing height. ω due to friction and orography have, of necessity, to fall off with height.

Fig. 7 (a,b) show the vertical profiles of ω due to various forcings on 7th near centres of ascent and descent. It is seen that the effect of dynamical forcings is larger, and they generally fall off with height.

We have also computed conversion from potential to kinetic energy associated with the Hadley and Walker circulations (Keshavamurty and Awade). Fig. 8 show the vertical profile of energy conversion from A_Z to K_Z during mean July, on 7 July 1963 and 19 July 1963. It shows that the total energy conversion is much larger on 7 July than in the mean and much smaller than the mean on 19 July 63, the weak monsoon day.

Fig. 9 (a,b,c) show y-p sections of energy conversion from A_E to K_E during mean July, 7 July and 19 July respectively. During mean July, there are regions of positive and negative conversions so that the net over the whole latitudinal belt becomes small. On 7 July, the strong monsoon day, there is a very large negative conversion (i.e. from K_E to A_E) mainly in the middle troposphere. This gives a net negative conversion over the whole latitudinal belt on 19 July, however, we have large positive conversion, mainly in the lower troposphere. This gives a net positive conversion.

Concluding remarks :

Computations using the quasi-geostrophic ω equation gives a smooth, consistent picture of the vertical circulations of the monsoon. The ω-field and the associated energy conversions show large fluctuations (from the mean) during contrasting monsoon epochs.

Acknowledgement :

The authors wish to express their grateful thanks to Dr.G.C.

... 7

Asnani, Dr. R. Ananthakrishnan and Shri S.K. Mishra for discussions and H.P. Das and M.B. Gajare for assistance in computation.

PGB/16.4.

R E F E R E N C E S

Berkofsky, L. and Bertoni, E.A.	1960	Topographic charts at one degree intersections for the entire earth. GRD Research Note No. 42.
Charney, J.G. and Eliassen, A.	1949	A numerical method for predicting the perturbation on the middle latitudes westerlies Tellus Vol.1.
Das, P.K.	1962	Mean vertical motion and non-adiabatic heat sources over India during the monsoon, Tellus, Vol.14, pp. 212-220.
Keshavamurty, R.N.	1971	On the maintenance of the mean monsoon circulation and the structure and energetics of monsoon disturbances Ph.D. Thesis.
Keshavamurty, R.N. and Awade, S.T.	1972	Energy conversions during weak monsoon, presented to Drought Symposium 1972, Poona.
Koteswaram, P.	1960	The Asian summer monsoon and the general circulation over the tropic, Proc. Symp. Monsoon of the world, New Delhi, 1958, IMD, pp. 105-110.
Raman, C.R.V., Keshavamurty, R.N. Jambunathan, R. and Ramanathan, Y.	1965	Some aspects of meridional circulation over the Indian monsoon area; Proc. Symp. Met.Res.IIOE, Bombay, 1965.
Rao, Y.P.	1962	Meridional circulation associated with the monsoon of India : Ind.Jour.Met. and Geoph., Vol.13, No.2, pp.157-166.
Rao, K.V. and Rajamani, S.	1968	Diagnostic study of a monsoon depression by geostrophic baroclinic model : Scientific Report No.54, Indian Institute of Tropical Meteorology, Poona-5.
Saha, K.R.	1968	Disturbances of vertical velocity in the monsoon field and structure of the monsoon circulation, Tellus, Vol.20, pp. 601-620.

***

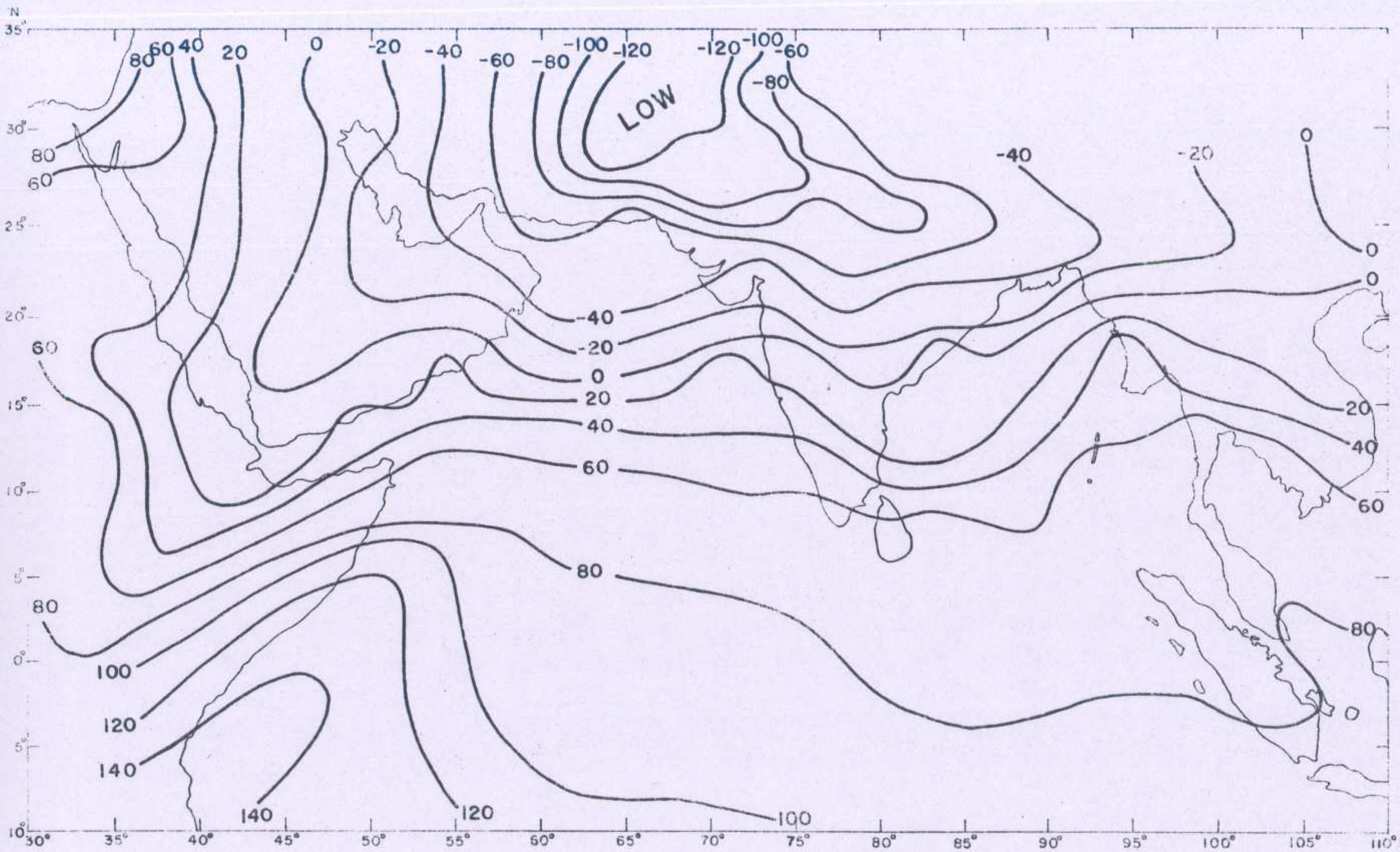

FIG.1(a) 1000 MB HEIGHT FIELD (GPM). 7-7-63.

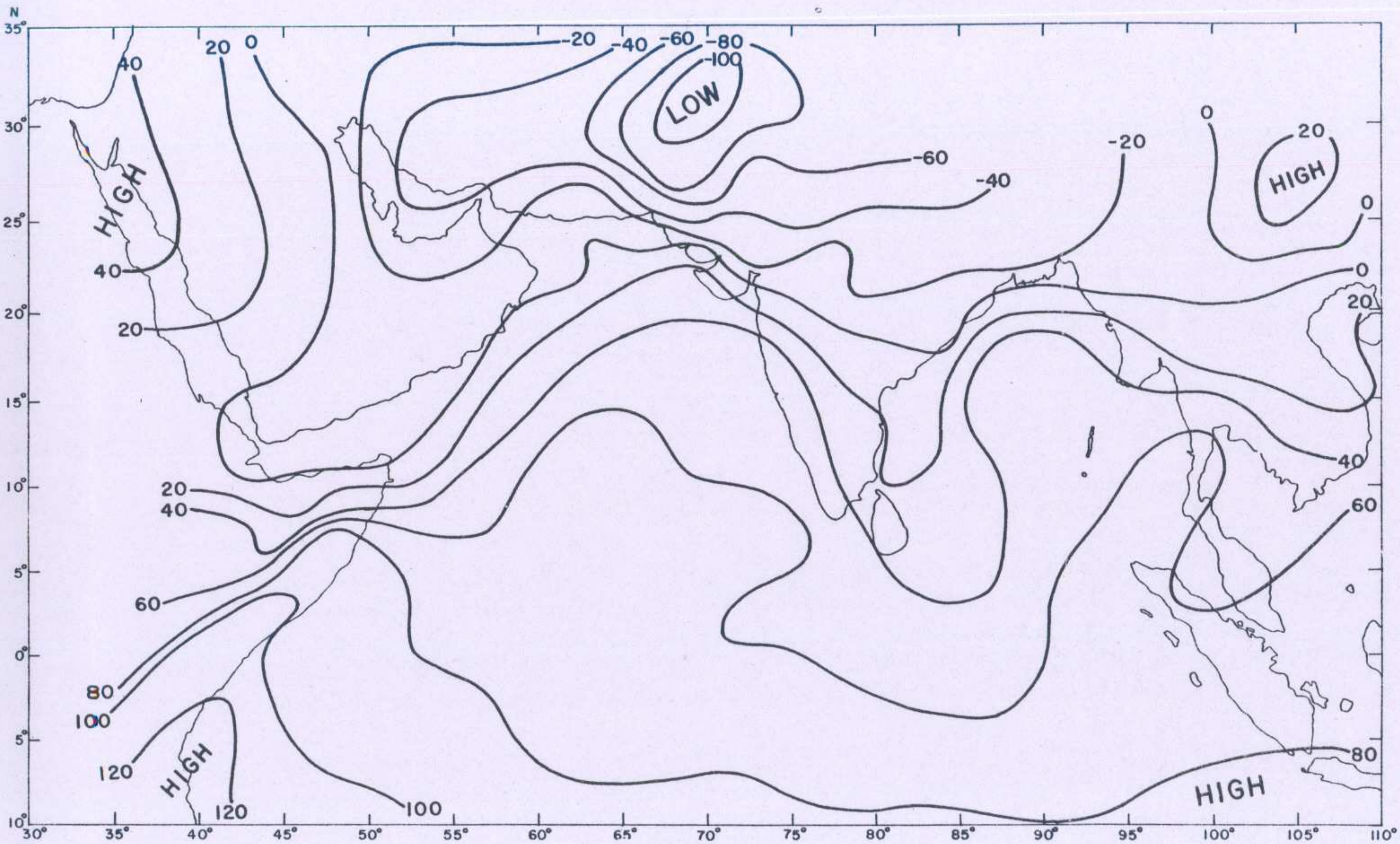

FIG. 1. 1000 MB HEIGHT FIELD (GPM). 19-7-63.

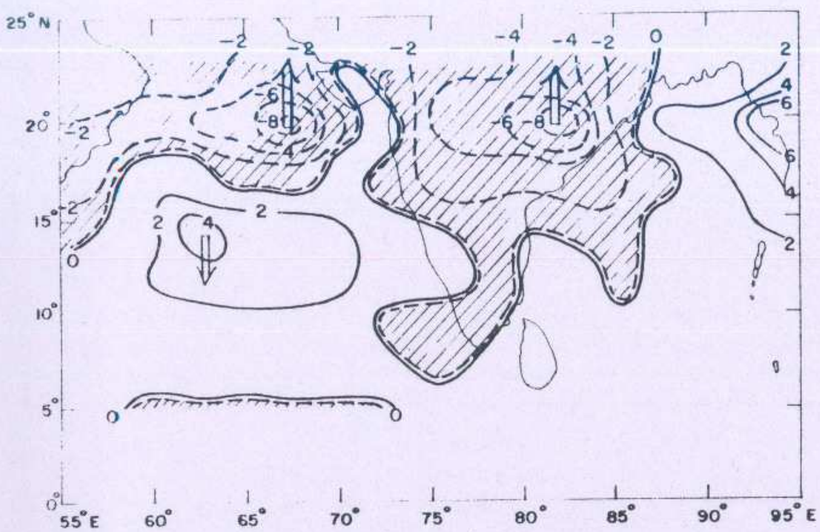

Fig.2 (a). ω due to all (10^{-4} mb Sec^{-1}), 850 mb, mean July

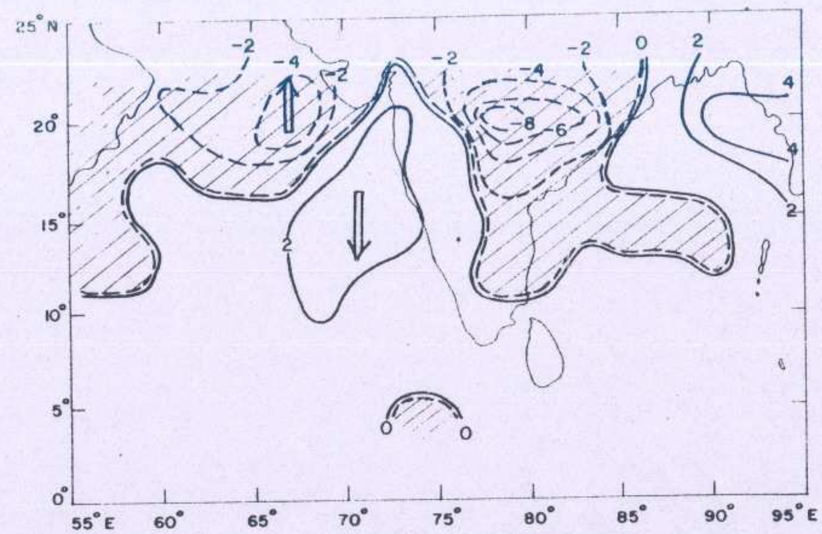

Fig.2(b). ω due to all (10^{-4} mb Sec^{-1}), 700 mb, mean july

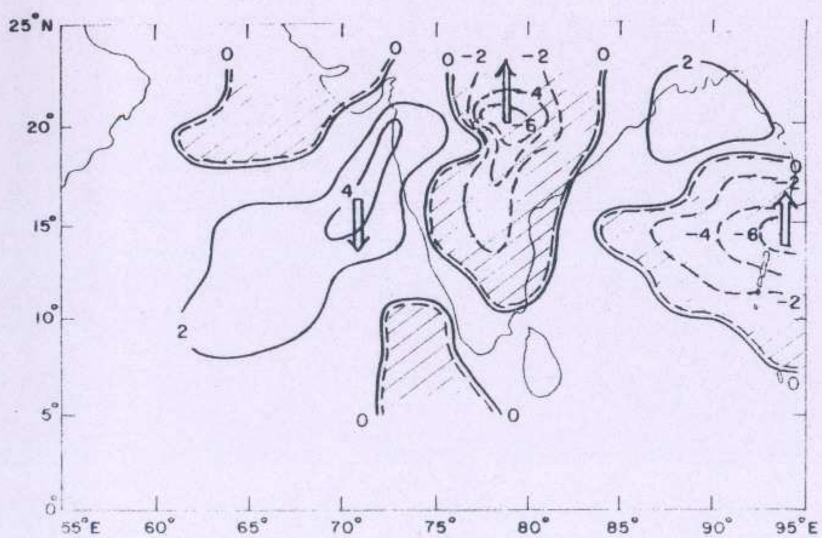

Fig.2(c). ω due to all (10^{-4} mb Sec^{-1}), 500 mb, mean july

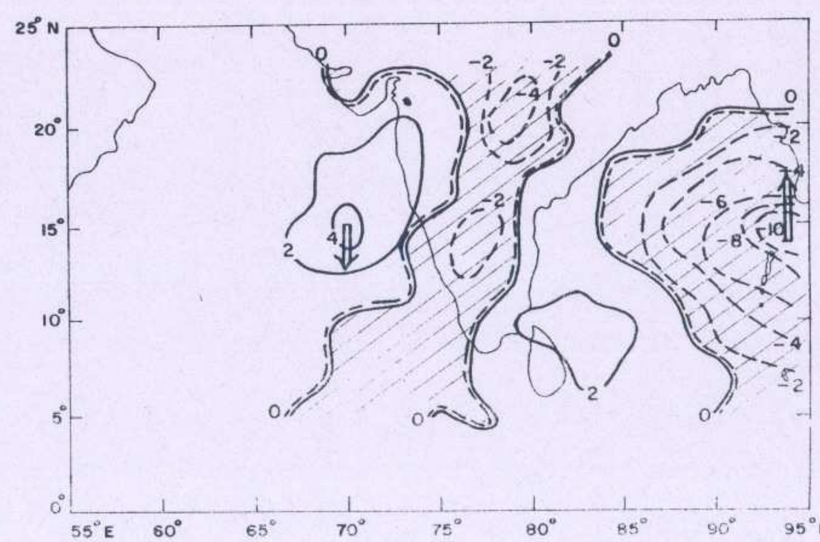

Fig.2(d). ω due to all (10^{-4} mb Sec^{-1}), 300 mb, mean july

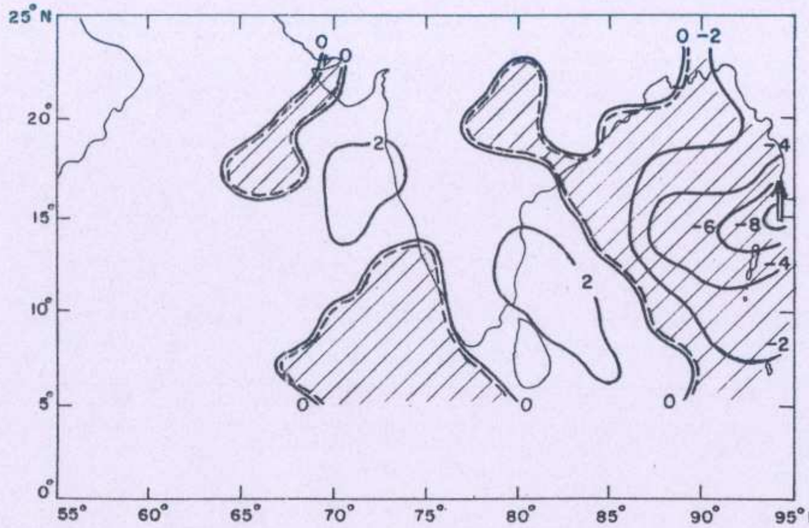

Fig.2(e). ω due to all (10^{-4} mb Sec.), 200 mb, mean july

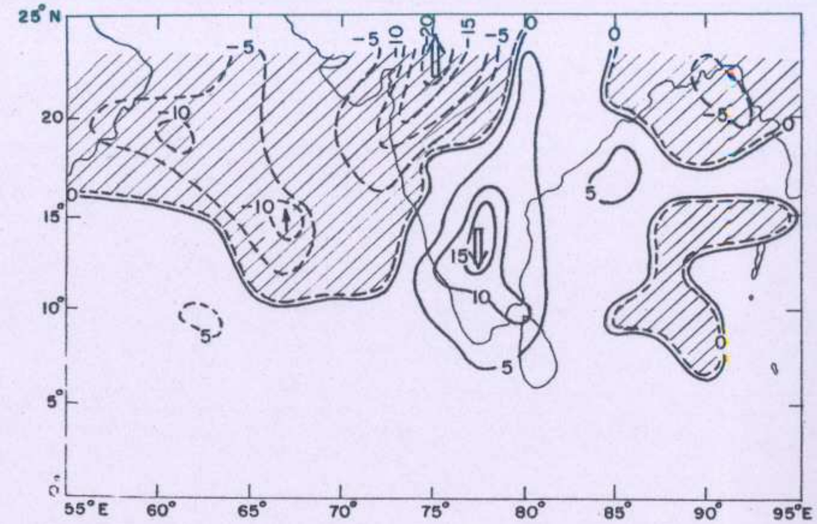

Fig.3(a). ω due to all (10^{-4} mb Sec^{-1}), 850 mb, 7th July, 1963

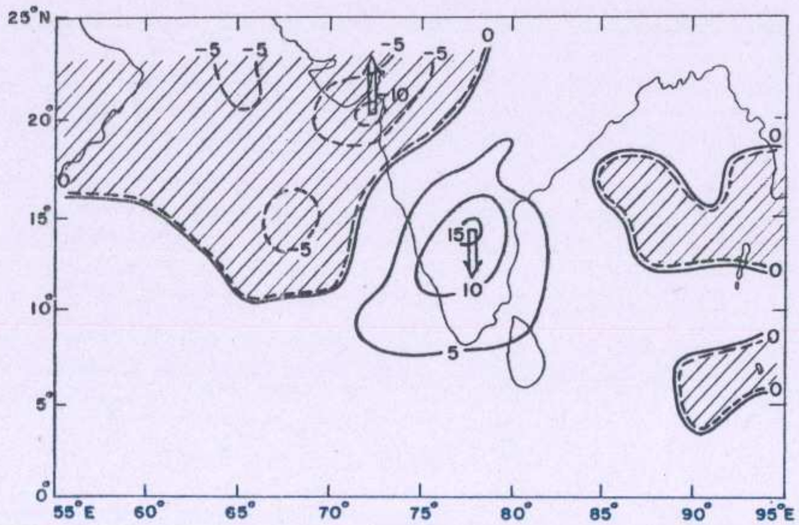

Fig.3(b). ω due to all (10^{-4} mb Sec^{-1}), 700mb, 7th July, 1963.

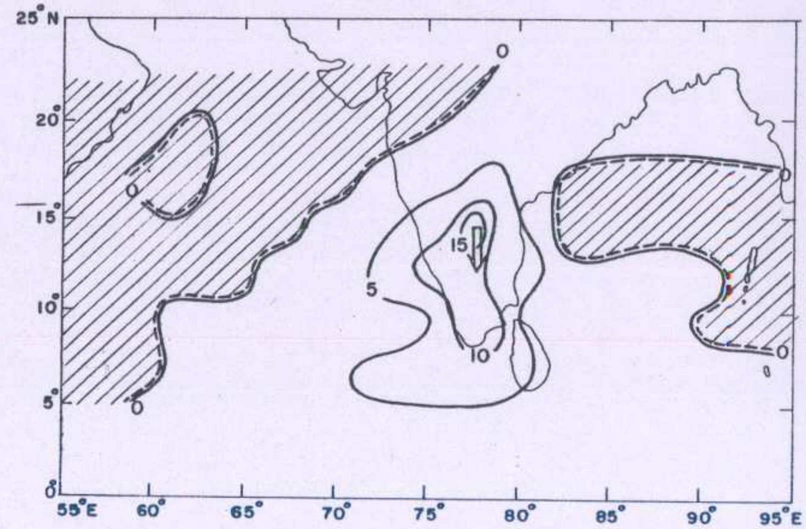

Fig.3(c). ω due to all (10^{-4} mb Sec^{-1}), 500mb, 7th July, 1963.

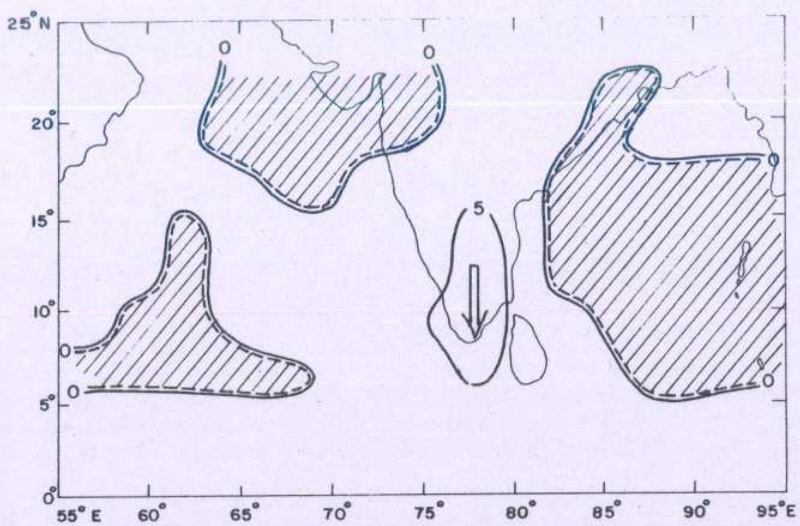

Fig. 3 (d). ω due to all (10^{-4} mb Sec^{-1}), 300 mb, 7th July, 1963.

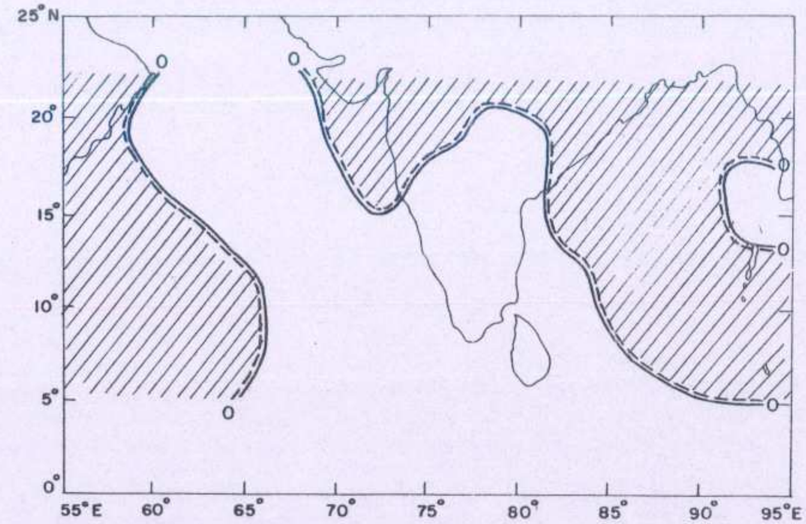

Fig. 3 (e). ω due to all (10^{-4} mb Sec^{-1}), 200 mb, 7th July, 1963.

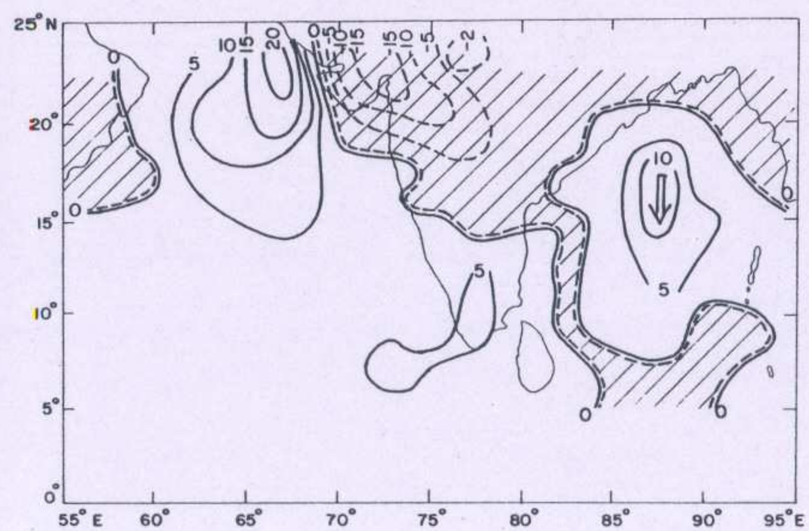

Fig. 4(a). ω due to all (10^{-4} mb Sec^{-1}), 850 mb, 19th JULY, 1963.

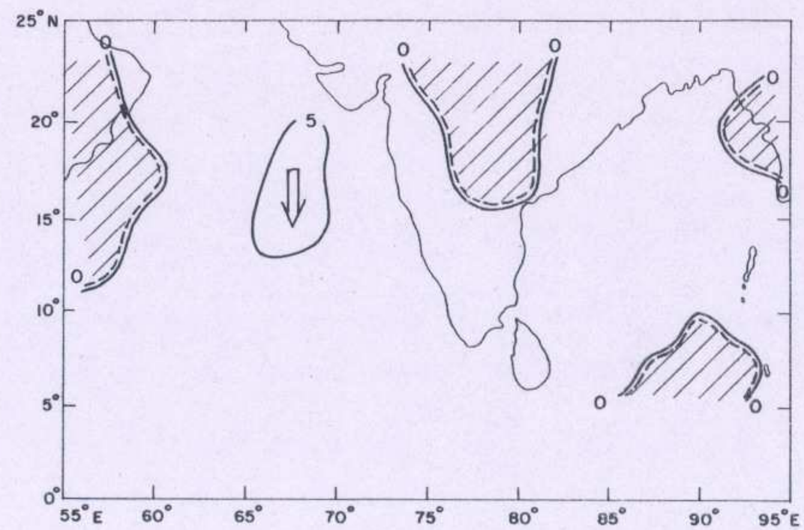

Fig. 4(b). ω due to all (10^{-4} mb Sec^{-1}), 700 mb, 19th July, 1963

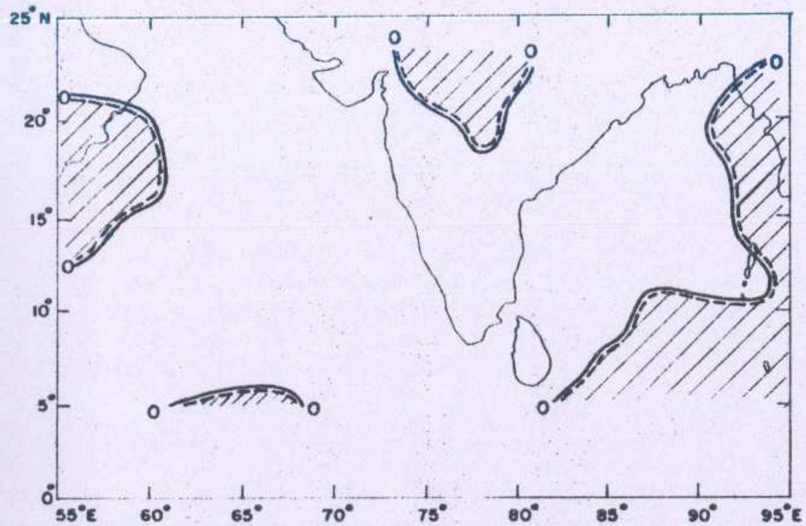

Fig. 4 (c). ω due to all (10^{-4} mb Sec^{-1}), 500 mb, 19th July, 1963

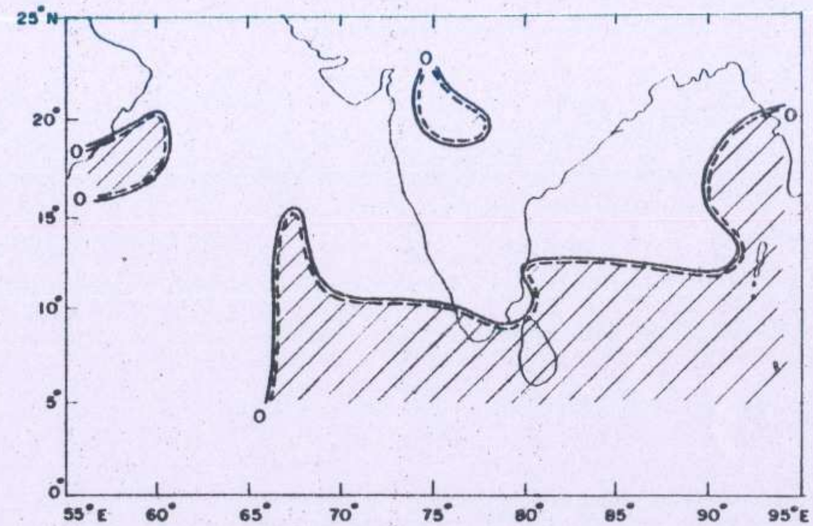

Fig. 4 (d). ω due to all (10^{-4} mb Sec^{-1}), 300 mb, 19th July, 1963

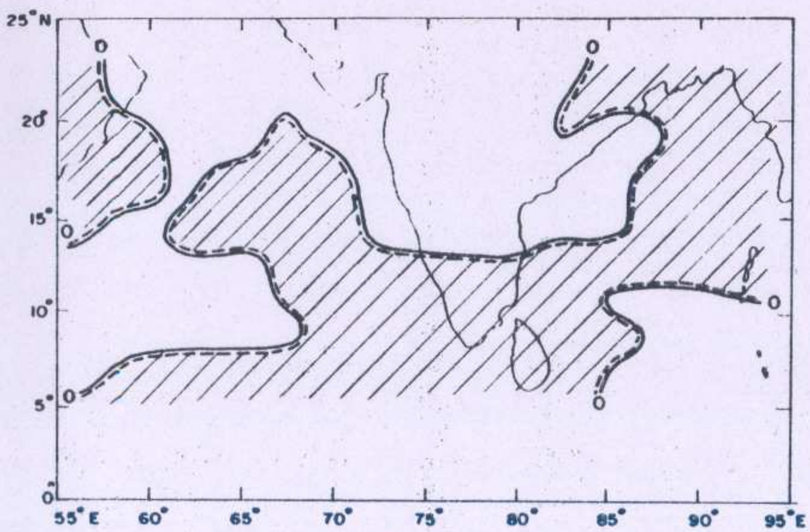

Fig. 4 (e), ω due to all (10^{-4} mb Sec^{-1}), 200 mb, 19th July, 1963

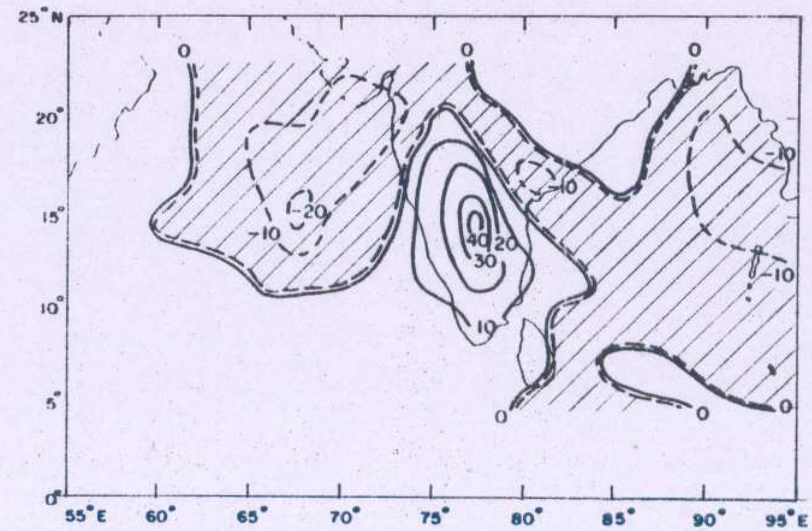

Fig. 5 (a), ω due to thermal advection (10^{-4} mb Sec^{-1}), 850 mb, 7th July, 1963

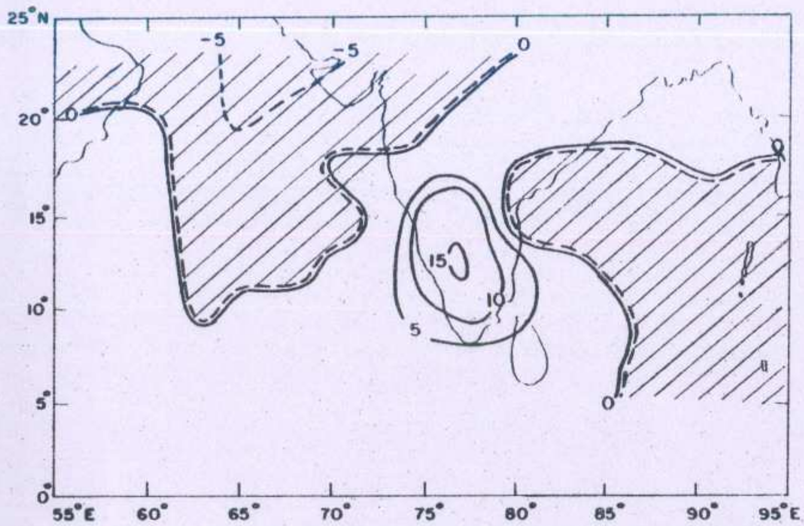

Fig.5(b). ω due to thermal advection (10^{-4} mb Sec^{-1}), 700 mb, 7th JULY, 1963

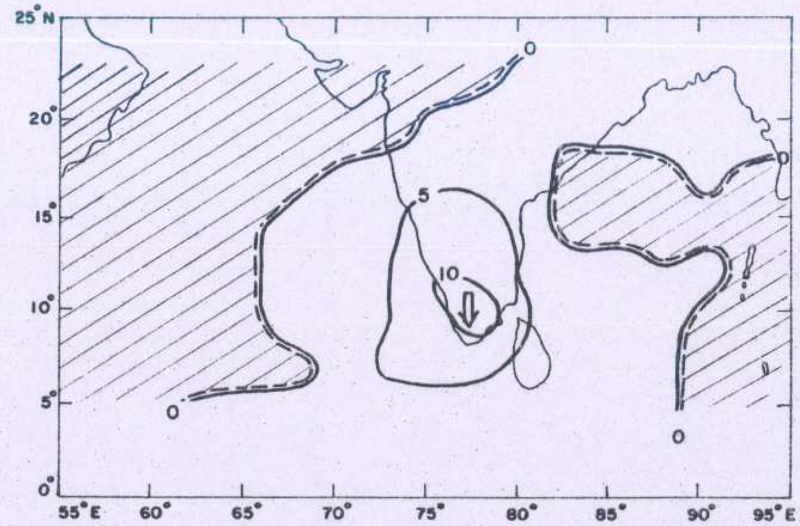

Fig.5(c). ω due to thermal advection (10^{-4} mb Sec^{-1}), 500 mb, 7th JULY, 1963.

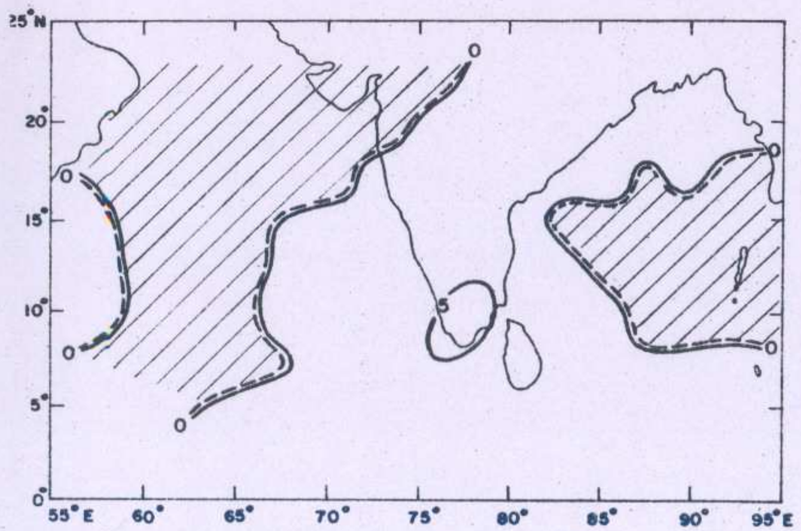

Fig. 5(d). ω due to thermal advection(10^{-4} mb Sec^{-1}), 300 mb, 7th JULY, 1963.

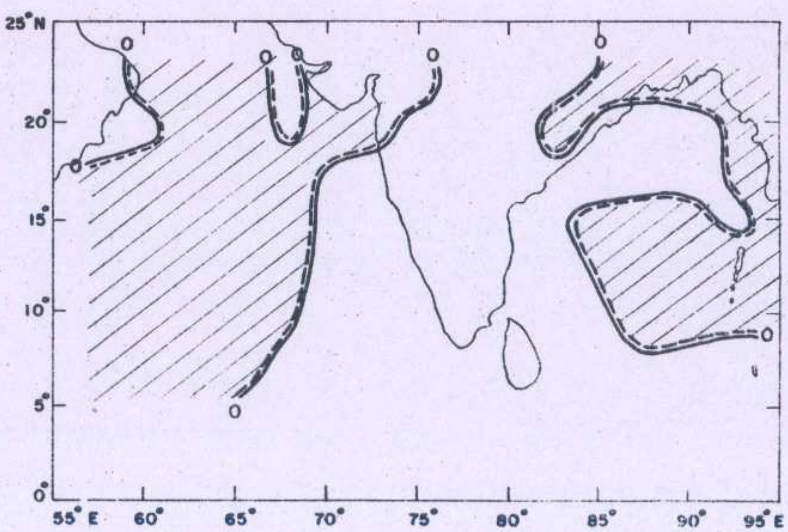

Fig.5(e). ω due to thermal advection (10^{-4} mb Sec^{-1}), 200 mb, 7th JULY, 1963.

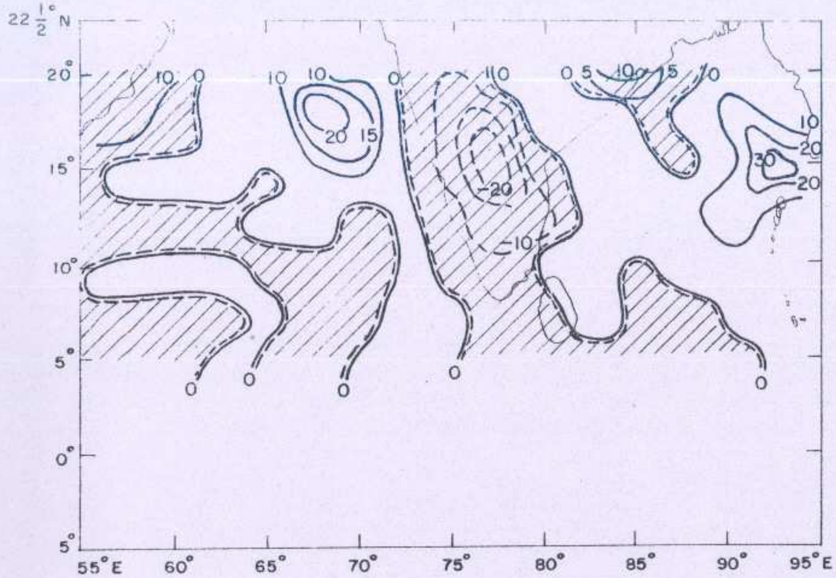

Fig.6(a). ω due to vorticity advection (10^{-4} mb Sec^{-1}), 850 mb, 7th JULY, 1963.

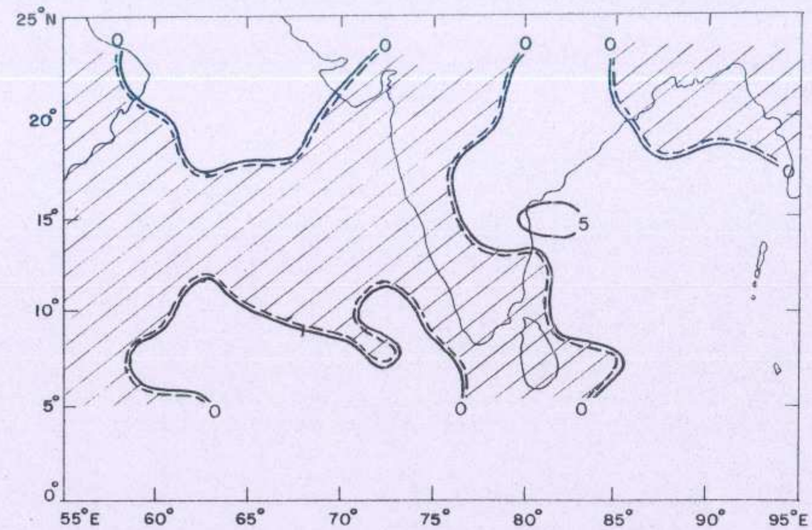

Fig.6(b) ω due to vorticity advection (10^{-4} mb Sec^{-1}), 700 mb, 7th JULY 1963.

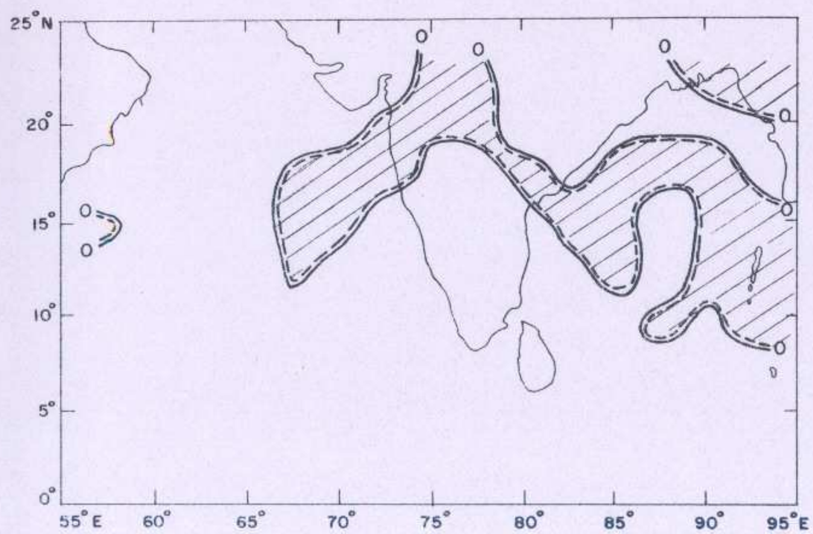

Fig.6(c). ω due to vorticity advection (10^{-4} mb Sec^{-1}), 500 mb, 7th JULY, 1963.

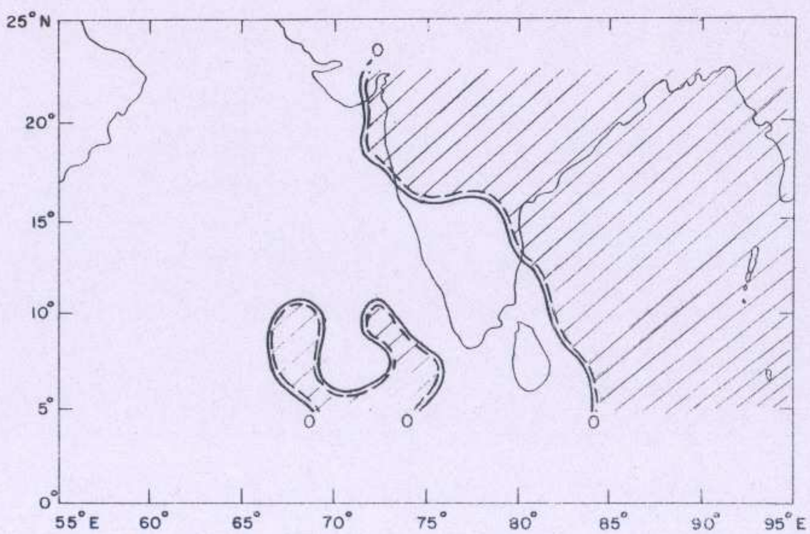

Fig.6(d). ω due to vorticity advection (10^{-4} mb Sec^{-1}), 300 mb, 7th July, 1963

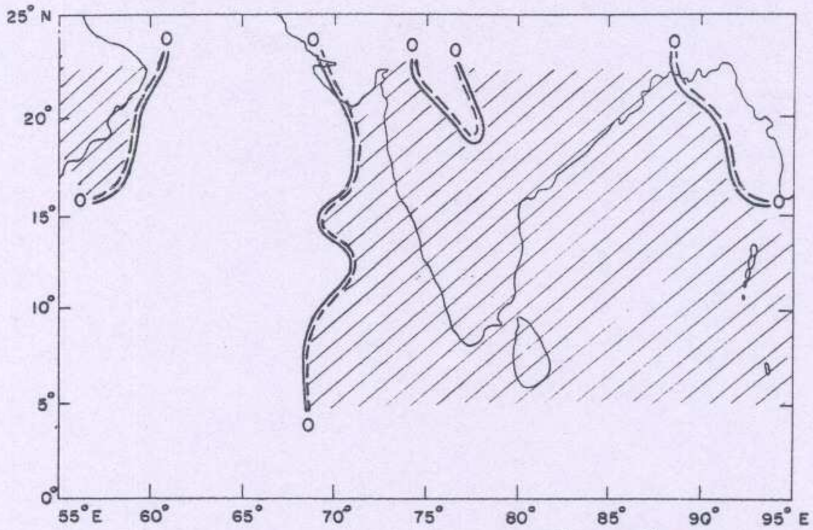

Fig.6 (e). ω due to vorticity advection, (10^{-4} mb Sec^{-1}), 200 mb, 7th July, 1963.

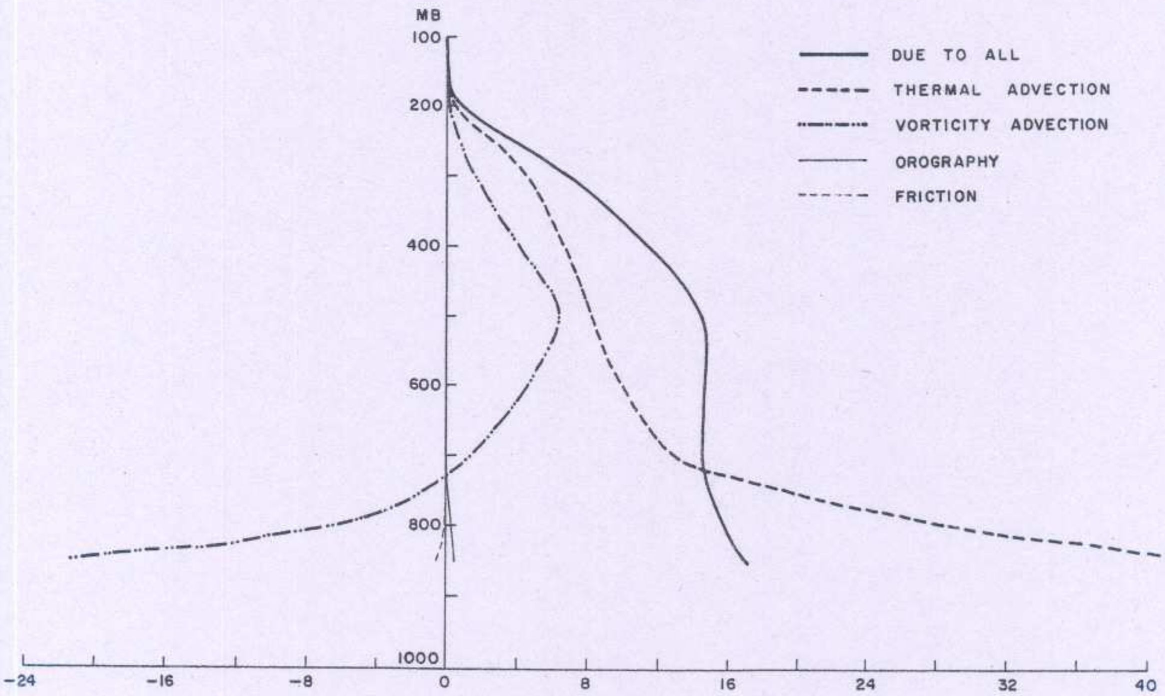

Fig.7 (a). ω due to various forcings at 15° N, 77$\frac{1}{2}$° E, 7th July, 1963

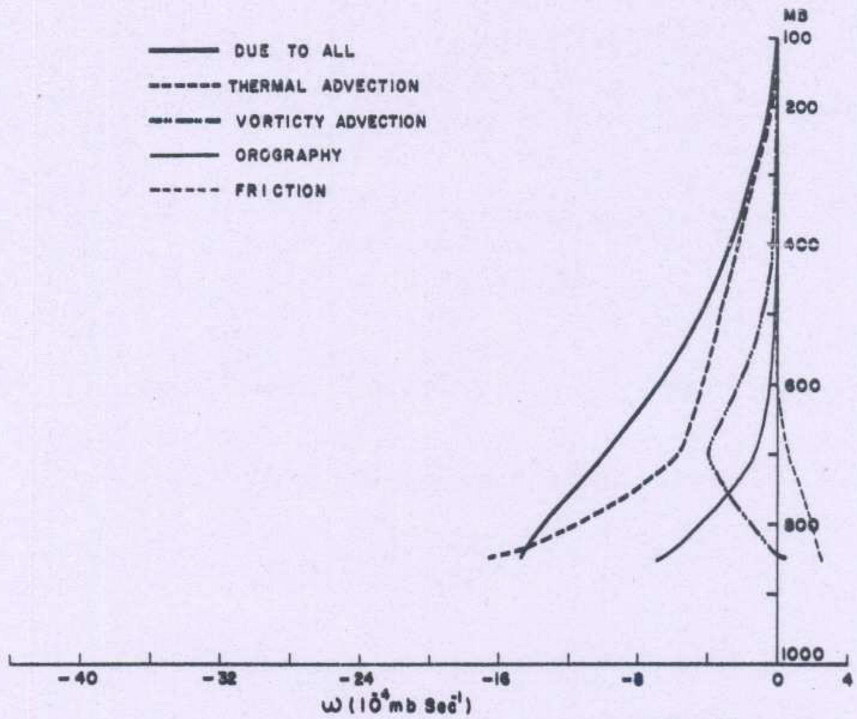

Fig.7 (b). ω due to various forcings at 20°N, 72½°E, 7th July, 1963

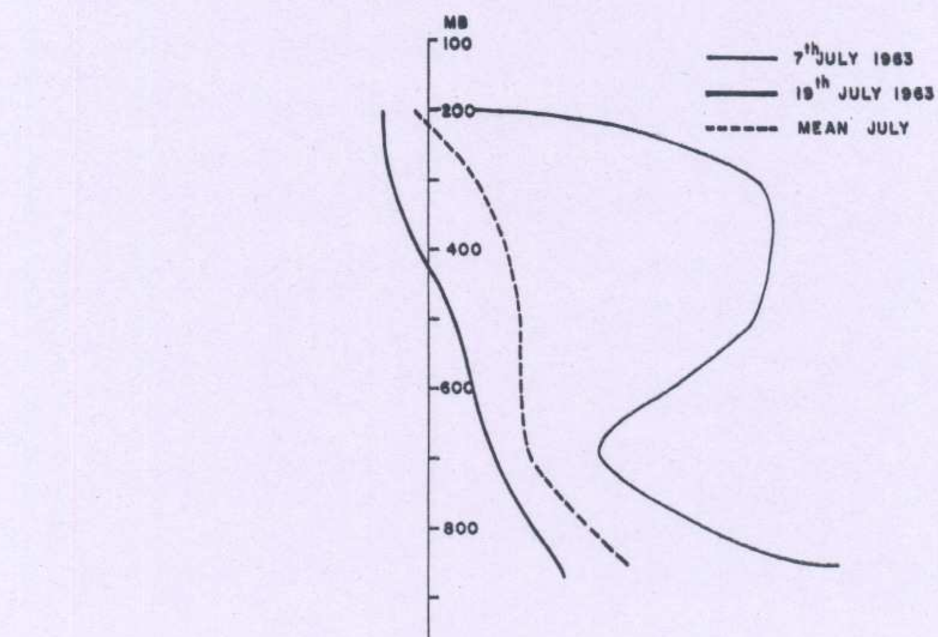

Fig.8. Values of $-[\omega]''[\alpha]''$ in units of 10^{-5} m^2 Sec^{-3}

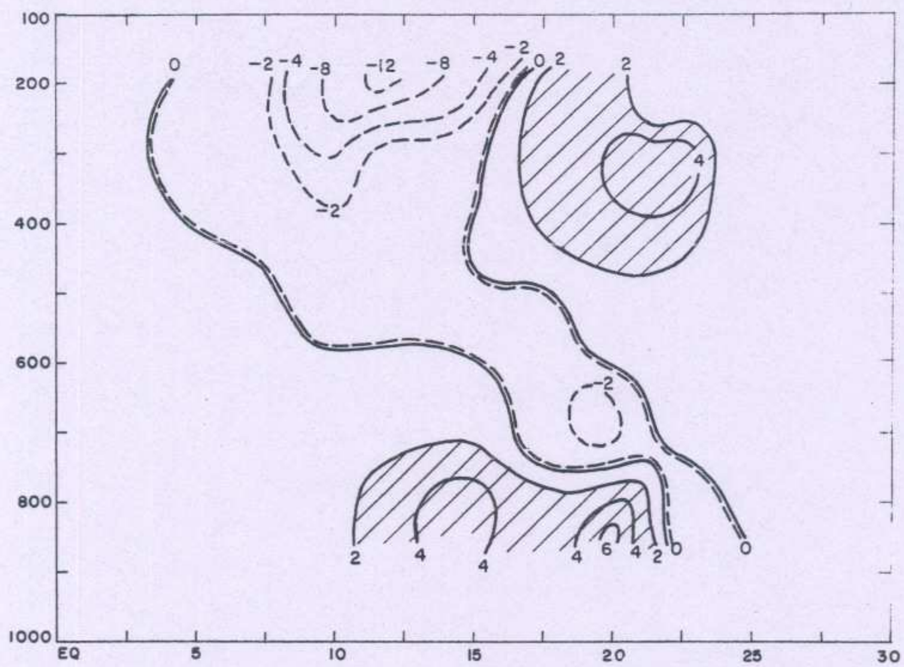

Fig. 9 (a). Mean height data, JULY
$-[\omega^*\alpha^*]$ in units of $10^{-5} m^2 Sec^{-3}$

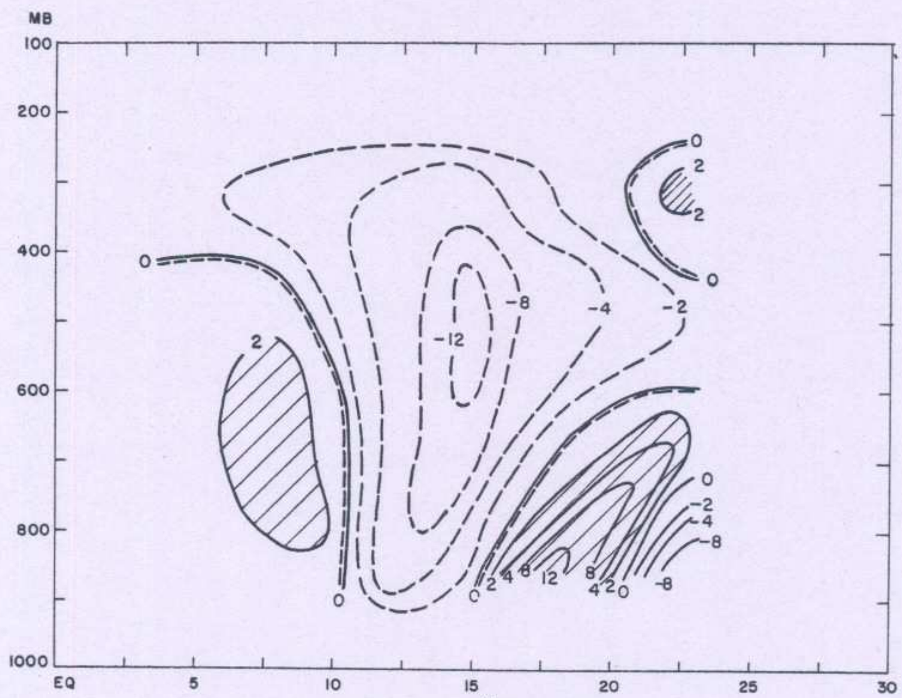

Fig. 9 (b). 7th July, 1963
$-[\omega^*\alpha^*]$ in units of $10^{-5} m^2 Sec^{-3}$

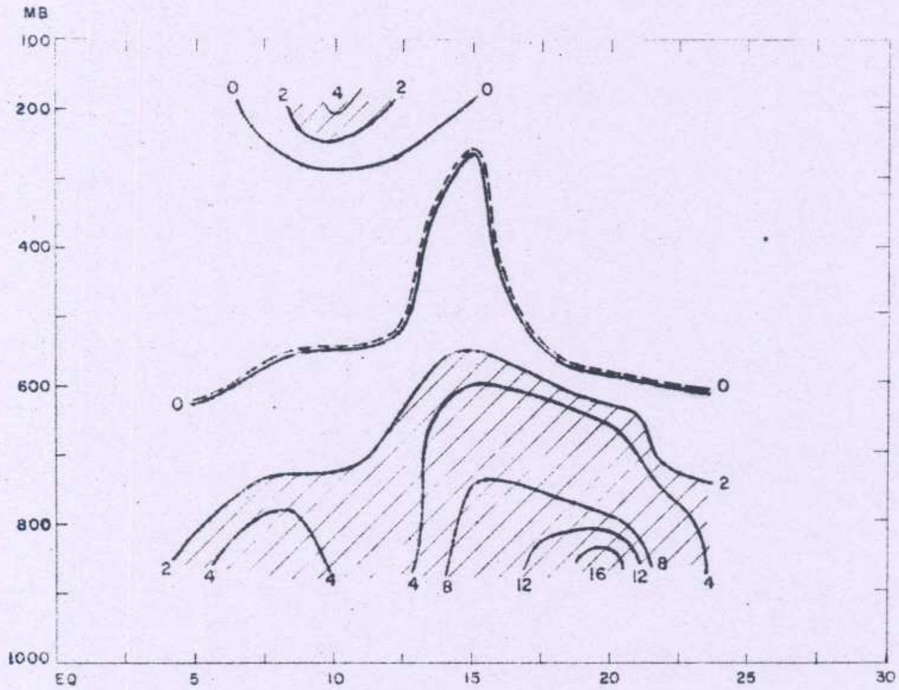

Fig.9 (c). 19th July, 1963
$-[\omega^{\circ}\alpha^{\circ}]$ in units of $10^{-5} m^2 Sec^{-3}$